Chinese Chemical Letters 36 (2025) 110059

Contents lists available at ScienceDirect

Chinese Chemical Letters

journal homepage: www.elsevier.com/locate/cclet

Enzyme-based colorimetric signal amplification strategy in lateral flow immunoassay

Haijiang Gong[a,1], Qingtan Zeng[b,1], Shili Gai[a,c,*], Yaqian Du[a], Jing Zhang[a], Qingyu Wang[a], He Ding[a,*], Lichun Wu[d,*], Anees Ahmad Ansari[e], Piaoping Yang[a,c,*]

[a] Key Laboratory of Superlight Materials and Surface Technology, Ministry of Education, College of Materials Science and Chemical Engineering, Harbin Engineering University, Harbin 150001, China
[b] Changhai Hospital Affiliated to Navy Military Medical University, Shanghai 200086, China
[c] Yantai Research Institute, Harbin Engineering University, Yantai 264000, China
[d] Department of Clinical Laboratory, Sichuan Cancer Hospital & Institute, Sichuan Cancer Center, School of Medicine, University of Electronic Science and Technology of China, Chengdu 611731, China
[e] King Abdullah Institute for Nanotechnology, King Saud University, Riyadh 11451, Saudi Arabia

ARTICLE INFO

Article history:
Received 22 March 2024
Revised 24 May 2024
Accepted 27 May 2024
Available online 1 June 2024

Keywords:
Lateral flow immunoassay
Signal amplification
Enzyme-based enhancement
Catalysis
Colorimetric signal

ABSTRACT

Lateral flow immunoassay (LFIA), a rapid detection technique noted for simplicity and economy, has showcased indispensable applicability in diverse domains such as disease screening, food safety, and environmental monitoring. Nevertheless, challenges still exist in detecting ultra-low concentration analytes due to the inherent sensitivity limitations of LFIA. Recently, significant advances have been achieved by integrating enzyme activity probes and transforming LFIA into a highly sensitive tool for rapidly detecting trace analyte concentrations. Specifically, modifying natural enzymes or engineered nanozymes allows them to function as immune probes, directly catalyzing the production of signal molecules or indirectly initiating enzyme activity. Therefore, the signal intensity and detection sensitivity of LFIA are markedly elevated. The present review undertakes a comprehensive examination of pertinent research literature, offering a systematic analysis of recently proposed enzyme-based signal amplification strategies. By way of comparative assessment, the merits and demerits of current approaches are delineated, along with the identification of research avenues that still need to be explored. It is anticipated that this critical overview will garner considerable attention within the biomedical and materials science communities, providing valuable direction and insight toward the advancement of high-performance LFIA technologies.

1. Introduction

The immunological analysis method based on antigen-antibody molecular recognition has been widely used in clinical diagnosis [1-4], food safety [5-8], environmental monitoring [9], and other fields due to the properties of high throughput, low expense, and simple operation [10,11]. Traditional immunological analysis techniques mainly include lateral flow immunoassay (LFIA) and enzyme-linked immunosorbent assay (ELISA). Among them, LFIA is highly valued in the field of point-of-care testing (POCT) due to the fast detection, low cost, and convenient use [5,12]. In LFIA technology, membranes with protein adsorption ability are used as carriers to fix the recognition molecules. Thus, signals can be generated between probes, analytes, and membrane-fixed recognition molecules through immune reactions [13]. As early as the 1980s, commercial human chorionic gonadotropin LFIA was already used for pregnancy response detection [14]. However, LFIA technology suffers from the low signal intensity in analyte detection, which limits its application in the fields requiring high sensitivity [15-17], such as early cancer diagnosis [18,19], metabolite detection [20,21], and toxin detection [22,23]. Therefore, it tends to develop suitable strategies and agents that amplify signal and enhance signal resolution capabilities to improve LFIA sensitivity.

Up to date, optimization was usually carried out in three directions: screening for high valence antibodies [24], controlling the flow of liquid to extend the reaction time [25-27], and enhancing the signal of immune probes [5,28,29]. Among them, the strat-

* Corresponding authors.
E-mail addresses: gaishili@hrbeu.edu.cn (S. Gai), dinghe@hrbeu.edu.cn (H. Ding), wulichun@scszlyy.org.cn (L. Wu), yangpiaoping@hrbeu.edu.cn (P. Yang).
[1] These authors contributed equally to this work.

https://doi.org/10.1016/j.cclet.2024.110059
1001-8417/

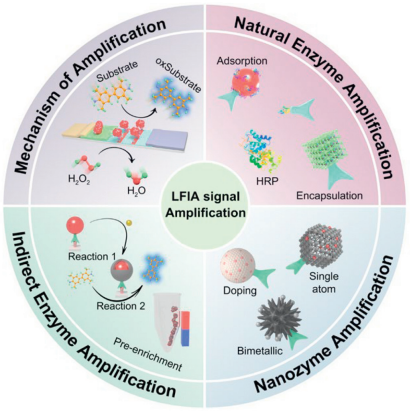

Fig. 1. Overview about enzyme-based colorimetric signal amplification in LFIA.

egy of optimizing antibodies required a lot of time and cost to obtain new antibodies with high valence [24], and the control of liquid flow put higher requirements on the production process of LFIA. Therefore, improving the signal strength by optimizing the immune probe became a promising solution. For example, gold nanoparticles (AuNPs) were widely used as a signal label for LFIA immune probes because of their vivid red color at specific sizes originating from the local surface plasmon resonance effect [30-32]. However, traditional colloidal gold has weak color intensity and cross-reactivity issues, which leads to limited sensitivity of LFIA detection [33,34].

Recently, to address the issues mentioned above, a variety of methods based on new immune probe labels were designed and studied, such as using an enzyme as a label to amplify the colorimetric signal [1,2,13,28], introducing a fluorescence signal to achieve signal amplification [35-38], adopting a sensitive surface-enhanced Raman scattering as the signal [39-41], and exploiting electromagnetic signal based on intrinsic properties of labels [42,43]. In addition, aptamers with higher robustness and sensitivity were used to replace antibodies in performing recognition functions, thereby enhancing detection accuracy [8,44]. The application of these methods showed high-intensity signals in LFIA, dramatically expanded the detection range of analytes, and solved the difficulties in detecting trace analytes [45,46]. However, there is a lack of accumulated studies about systematic introduction focused on mechanisms and progress of them. Therefore, the basic principles and design concepts of signal enhancement methods need to be summarized to provide guidance for the development of high-performance LFIA in the future.

Herein, the enzyme-based colorimetric signal amplification strategies in LFIA are focused in this review, and the amplification mechanism of enzyme labels are deeply expatiated (Fig. 1). Then, enzyme-based signal amplification methods are also systematically sorted out and divided into direct signal amplification and indirect signal amplification. Direct signal amplification is referred to the utilization of natural enzymes or nanozymes as probes to directly catalyze the substrate reactions to form color changes, thereby achieving signal enhancement. Conversely, indirect signal amplification involves preprocessing samples (such as pre-enrichment) by exploiting the inherent characteristics of enzymatic probes, enhancing immune responses through increased enzyme activity, or establishing cascade reactions to indirectly augment the signal. Additionally, a comprehensive overview of the application scenarios of enzymatic activity labels in LFIA and novel enzymatic signal amplification technologies are provided. Finally, comments on existing amplification strategies and prospects for the development of

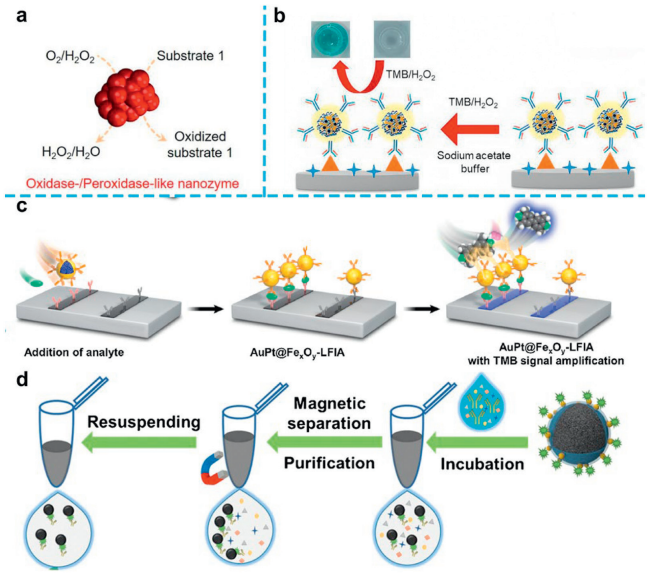

Fig. 2. The mechanism of enzymatic signal amplification strategy. (a) Substrate oxidized by H_2O_2 to form colored products in the presence of the enzyme. Reproduced with permission [63]. Copyright 2021, American Chemical Society. (b) Colorimetric detection by the nanozymes-based immunoassay. Reproduced with permission [64]. Copyright 2023, Elsevier Ltd. (c) Operating procedure for detection of cTnI *via* the AuPt@Fe_xO_y-LFIA. Reproduced with permission [54]. Copyright 2023, Elsevier B.V. (d) Diagram of the detection principle for detecting human severe acute respiratory syndrome coronavirus-2-N protein antibody using Fe_3O_4-Ag^{MBA}@Au NPs. Reproduced with permission [65]. Copyright 2022, Springer-Verlag GmbH Germany.

enzyme-based signal amplification in LFIA are concluded, emphasizing future pathways and promising directions in this dynamic field.

2. Mechanism of enzyme-based signal amplification

Enzymes are catalysts that accurately accelerate reactions of specific substrates, making them excellent for signal amplification in LFIA due to their high selectivity (Fig. 2) [47]. They catalyze substrate oxidation for colorimetric signals, like horseradish peroxidase (HRP) oxidizing 3,3′,5,5′-tetramethylbenzidine (TMB) to generate a strong absorbance signal (Figs. 2a and b) [13,48,49]. Enzyme activity probes in LFIA signal amplification involve direct and indirect strategies. Direct amplification replaces gold nanoparticles with enzyme or nanozyme probes that catalyze substrate oxidation, resulting in the colorimetric signal enhancement (Fig. 2c) [9,10,13,50]. Natural enzyme probes are often use in bare designs or protective materials like metal-organic frameworks (MOFs) and hydrogels [11,51,52]. Nanozyme probes, categorized into simple and composite, play a key role in signal amplification [12,53,54]. Based on nanozyme inherent characteristics, they can combine with colorimetric signals to form multiple signals and calibrate errors from environmental or chemical factors [55-57]. Indirect signal amplification strategies include analyte pre-enrichment and cascade reactions [58,59]. Pre-enrichment strategies utilize the magnetic properties of nanozymes to concentrate analytes from samples, followed by chromatography and direct signal amplification (Fig. 2d) [60]. Cascade reaction systems are created by generating or attaching enzymatically active units on captured probes, enable multistage amplification for high-intensity signal output [61-65]. Both direct and indirect amplification methods have been explored, with representative enzymes and outcomes summarized in Table 1 [1,6,11,16,17,28,29,58-62,66-75].

Table 1
Representative enzymes and outcomes used in LFIA.

Amplification method	Sample	Outcomes (H_2O_2 as substrate)	Analytes	Detection time	LODs and linear ranges	Ref.
Direct enzyme-based amplification	Pt@AuNF-HRP	$K_m = 0.285$ mmol/L $V_{max} = 1.45\times10^{-6}$ mol L^{-1} s^{-1} (Pt@AuNF only)	Zearalenone	—	0.052 ng/mL 0.52–7.21 ng/mL	[17]
	MPs-GAMI-HRP	—	Microcystin-leucine-arginine	17 min	0.002 ng/mL 0.0337–0.0037 ng/mL	[66]
	HRP-AuNPs	—	Hemoglobin A1c	26 min	3.3% 3.3%−15.1%	[16]
	(HRP@ZIF-8)^3@PDA@HRP	$K_m = 3.70$ mmol/L $V_{max} = 8.71\times10^{-8}$ mol L^{-1} s^{-1}	Cardiac troponin I	26 min	0.01 ng/mL	[11]
	CRIs-gel	—	Target DNA	35 min	2 copies/μL	[67]
	Chiral-PAD	—	L/D-Lactate	30 min	30 μmol/L; 3 μmol/L 0.1–3.0 mmol/L; 0.01–0.5 mmol/L	[68]
	Pt-Ru NCs	115.36 U/mg	D-dimer	20 min	1 ng/mL	[69]
	Pd@Ir NPs	$K_m = 0.246$ mmol/L $K_{cat} = 4.36\times10^{-5}$ s^{-1}	Pepsinogen I/II	6 min	0.01 ng/mL 0.01–10 ng/mL	[70]
	pPtNZ	$K_m = 7.04$ mmol/L $V_{max} = 8.92\times10^{-7}$ mol L^{-1} s^{-1}	C-reactive protein	20 min	0.03 ng/mL 0.1–1000 ng/mL	[1]
	Fe-N-C SAzyme	$K_m = 0.191$ mmol/L $V_{max} = 1.506\times10^{-6}$ mol L^{-1} s^{-1}	Fumonisin B_1/aflatoxin B_1	—	0.0139 ng/mL; 0.0028 ng/mL 0.02–150 ng/mL; 0.005–200 ng/mL	[28]
	FTAN	$K_m = 3.50$ mmol/L $V_{max} = 1.311\times10^{-7}$ mol L^{-1} s^{-1}	Ractopamine/clenbuterol	—	0.015 ng/mL; 0.156 ng/mL 0–1 ng/mL; 0–10 ng/mL	[6]
	VS_2NS	$K_m = 0.40$ mmol/L	17β-Estradio	7 min	0.406 ng/mL 0–15 ng/mL	[29]
	PCu	$K_m = 0.13$ mmol/L $V_{max} = 1.12\times10^{-7}$ mol L^{-1} s^{-1}	*Aspergillus flavus*	9 min	0.22 ng/mL	[71]
	Co doped g-C_3N_4	$K_m = 0.678$ mmol/L $V_{max} = 1.39\times10^{-9}$ mol L^{-1} s^{-1}	Hypoxanthine	25 min	1.52 mg/kg 1.7–272.2 mg/kg	[72]
	AuAg@PB MOF	$K_m = 0.015$ mmol/L $V_{max} = 1.52\times10^{-7}$ mol L^{-1} s^{-1}	*E. coli* and *S. aureus*	10 min	6 CFU/mL	[73]
	Au@PBNP	$K_m = 2.983$ mmol/L $V_{max} = 8.9732\times10^{-7}$ mol L^{-1} s^{-1}	Alpha-lactalbumin	60 min	0.011 ng/mL 0.2–600 ng/mL	[74]
Indirect enzyme-based amplification	Fe_3O_4@PDA@Pt	$K_m = 0.459$ mmol/L	*Escherichia coli* O157:H7	10 min	10 CFU/mL —	[58]
	Fe_3O_4@MOF@Pt	$K_m = 12.5$ mmol/L $V_{max} = 2.174\times10^{-7}$ mol L^{-1} s^{-1}	Procalcitonin	25.5 min	0.0005 ng/mL 0.0005 ng/mL– 0.136 ng/mL	[59]
	$NiCo_2O$	—	17β-Estradiol	10 min	0.2 ng/mL 0–8 ng/mL	[60]
	TsAIP	—	Furazolidone	10 min	1 ng/mL 0–3 ng/mL	[75]
	Au@Au	$K_m = 0.16$ mmol/L $V_{max} = 2.016\times10^{-7}$ mol L^{-1} s^{-1}	*E. coli*	37 min	1.25×10^1 CFU/mL 12.5–1.25×10^5 CFU/mL	[62]
	PBNCD	—	Aflatoxin B_1	58 min	0.023 ng/mL 0.006–0.09 ng/mL	[61]

3. Direct signal amplification strategies

3.1. Natural-enzyme-based signal amplification strategies

Natural enzymes are a class of efficient biocatalysts with high selectivity and activity. Typically, HRP is particularly common in enzyme-based signal amplification methods [76]. HRP can effectively catalyze the chromogenic reactions of peroxidase (POD) substrates, such as TMB [77], *o*-phenylenediamine (OPD) [78], 2,2′-azinobis-(3-ethylbenzthiazoline-6-sulphonate) (ABTS) [79], and 3-amino-9-ethylcarbazole (AEC) [80].

The excellent performance of HRP results in widely used in ELISA [81-83] and considered as an essential tool for signal amplification in LFIA [16,17,66]. In this part, the application of natural enzymes in LFIA will be discussed in detail, and the methods will be divided into two categories: exposed natural enzymes by carriers and protected natural enzymes by biomineralization.

3.1.1. Exposed natural enzymes by carriers

The natural enzyme loaded on the carrier is modified with an immune recognition device. Typically, the carrier can be noble metal nanoparticles [48,84], nanozymes with synergistic effects [17,80], and magnetic microspheres [66]. Qiao *et al*. designed and prepared a composite enzyme probe that adsorbs HRP onto the surface of Pt@Au nanoflowers for high-sensitivity detection of zearalenone (ZEN) [17]. Prepared nanoflower morphologies were depicted in Figs. 3a and b. The synergy of Pt@Au nanoflowers with HRP was leveraged to enhance TMB oxidation based on POD activity. The probe boosted signal intensity *via in situ* TMB oxidation at test/control (T/C) lines (Fig. 3c), achieving a 6-fold signal amplification (Fig. 3d). The LFIA was with a limit of detection (LOD) of 0.065 ng/mL and a detection range of 0.065–1.418 ng/mL. After signal amplification, LOD was as low as 0.052 ng/mL, extending the range to 0.052–7.28 ng/mL. This LFIA matched fluorescence-based LFIA performance while offering broader colorimetric signal applicability.

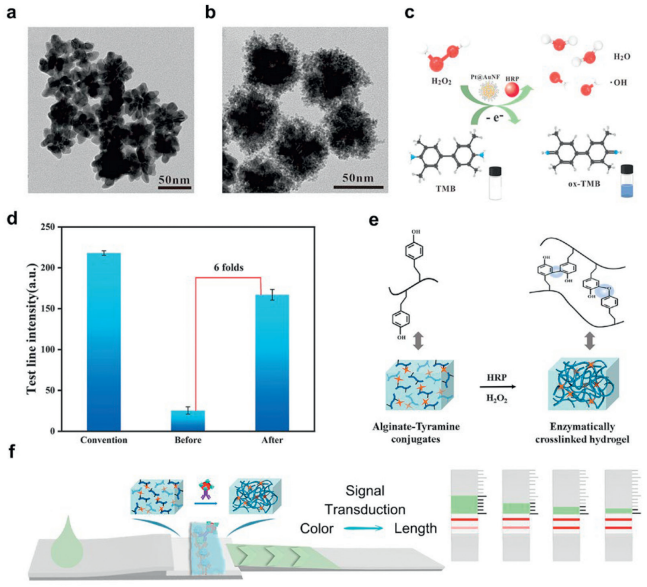

Fig. 3. Transmission electron microscopy images of (a) Au nanoflowers and (b) Pt@Au nanoflowers. (c) Schematic diagram of enzyme catalytic signal amplification of Pt@AuNF-HRP. (d) T line signal intensity of different probes. Reproduced with permission [17]. Copyright 2023, Elsevier B.V. (e) Schematic illustration of enzymatically cross-linking alginate-tyramine (Alg-Tyr) hydrogel formation. (f) Color-distance signal transduction mediated by HRP-Au Ab probe. Reproduced with permission [16]. Copyright 2023, American Chemical Society.

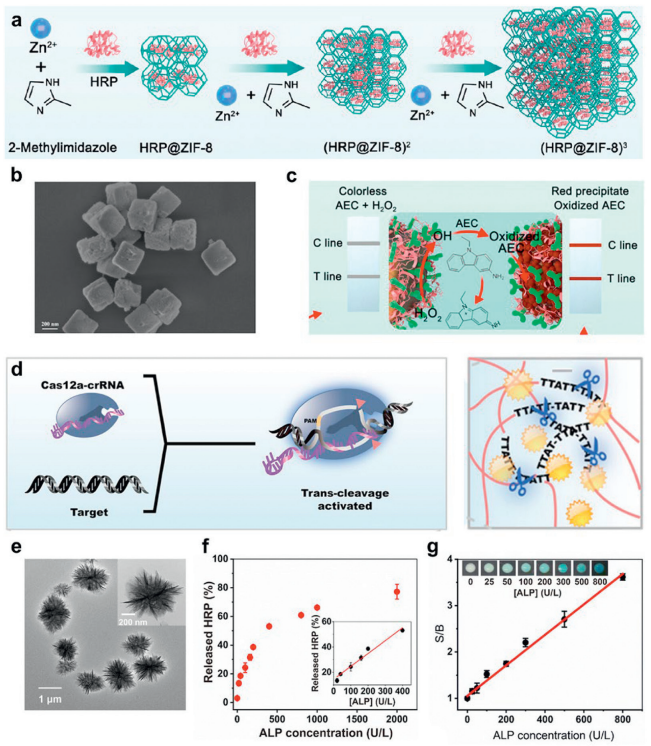

Fig. 4. (a) Schematic illustration of the synthetic process of $(HRP@ZIF\text{-}8)^3$. (b) Scanning electron microscopy images of $(HRP@ZIF\text{-}8)^3$@PDA. (c) The principle of enzymatic signal amplification by $(HRP@ZIF\text{-}8)^3$@PDA@Ab/HRP. Reproduced with permission [11]. Copyright 2023, American Chemical Society. (d) Schematic diagram of Cas12a-crRNA recognizing target DNA and splitting hydrogel. Reproduced with permission [67]. Copyright 2023, American Chemical Society. (e) Transmission electron microscopy images of HRP@3D DNA. (f) Relative released HRP (%) as a function of the concentration of ALP ($t = 20$ min). Inset: A linear dynamic range of 0–400 U/L ALP. (g) Signal-to-background (S/B) values for paper device carried out under different concentrations of ALP (0, 25, 50, 100, 200, 300, 500, and 800 U/L). Reproduced with permission [86]. Copyright 2023, The Royal Society of Chemistry.

Similarly, Olga *et al*. developed an enzyme label for the LFIA detection of microcystin-LR by immobilizing HRP onto the surface of magnetic nanoparticles (HRP-MPs-GAMI) [66]. Magnetic nanoparticles with a strong orange color were used as carriers for HRP, realizing the basic orange colorimetric signal and the signal amplified after catalysis. This method ultimately achieved an ultra-low LOD of 0.002 ng/mL for microcystin-LR. Besides, hydrogels catalyzed by HRP were used for LFIA to achieve signal transduction. Liu and co-workers utilized HRP-adsorbed AuNPs as enzymatic activity labels to realize the highly sensitive detection of hemoglobin A1c [16]. The HRP-responsive hydrogels were developed, which achieved transduction and amplification of colorimetric signals into length signals based on permeability changes induced by the interaction between the hydrogels and HRP (Figs. 3e and f). These permeability changes allowed varying degrees of water infiltration, resulting in wetting different lengths of the absorbing pad. This enabled the conversion of the colorimetric signal to a visually quantifiable length signal, achieving rapid and quantitative detection of specific proteins in samples using LFIA through visual observation.

In short, natural enzyme-based signal amplification probes can be prepared by fixing natural enzymes on the surface of carriers [85], which provide well-established solutions and streamlined preparation procedures. Nevertheless, the limited load capacity of the carriers imposes constraints on the improvement of signal amplification capabilities. Consequently, augmenting the natural enzyme loading amount on probes represents a pivotal solution for elevating the detection sensitivity of LFIA. Meanwhile, utilizing enzyme activity to convert signals into more easily interpretable signals is also a research hotspot.

3.1.2. Protected natural enzymes by biomineralization

The porous structures such as MOFs and hydrogels are used for the biomineralization of natural enzymes to offer a higher enzyme loading capacity compared to regular carriers, resulting in enzyme complexes that effectively preserve the activity of the natural enzymes. Consequently, this enhances the signal amplification capability. Song and co-workers developed a pomegranate-shaped enzyme-active label by encapsulating HRP within zeolite imidazolate framework-8 (ZIF-8) [11]. The catalytic activity of the label was enhanced by the porous framework, which provided a space for immobilizing HRP and facilitates substrate diffusion (Fig. 4a). The outer coating of polydopamine served as a scaffold for connecting antibodies and HRP while providing a vivid color, resulting in the final morphology depicted in Fig. 4b. Ultimately, this approach achieved a visually distinguishable sensitivity of 0.01 ng/mL for cardiac troponin I after catalyzed oxidation of AEC (Fig. 4c).

Zhao *et al.* developed a DNA-responsive hydrogel doped with amylase (GA) and human chorionic gonadotropin (hCG) for high-sensitivity target DNA detection [67]. Upon target DNA presence, the hydrogel was cleaved, and GA and hCG was released (Fig. 4d). This led to color fade and hCG detection *via* LFIA test strip to quantify the target DNA. The detection limit was reduced to 2 copies/μL. Additionally, Chang *et al.* designed a paper-based device integrating HRP-encapsulated 3D DNA for alkaline phosphatase (ALP) detection [86]. HRP molecules were encapsulated by DNA, forming flower-like HRP@3D DNA (Fig. 4e). The ALP presence could disrupt the structure, resulting in HRP exposure and colorimetric signals production. In this system, the release rate of HRP linearly correlated with ALP concentration (Fig. 4f). The paper-based sensor based on self-assembled HRP@3D DNA showed a strong linear relationship with ALP concentration (Fig. 4g), with a LOD of 13.4 U/L.

In signal amplification techniques, HRP is a preferred natural enzyme, widely applied in immunohistochemistry and immunoas-

say due to abundant raw materials and an established industrial chain. The traditional method of labeling HRP on secondary antibodies is challenging, with operational complexity and purification difficulties, resulting in high development costs. Alternatively, using a carrier aggregating HRP for antibody conjugation can simplify purification, accelerating immunoassay probe development. Natural enzymes efficient catalytic properties suggest potential as high-performance probes in LFIA. However, due to the nature of the HRP protein, external conditions such as pH and ion concentration have a significant impact on its activity. Consequently, LFIA utilizing HRP as the enzyme activity source is only suitable for the detection of analytes under mild sample conditions, and drastic changes in sample conditions may significantly affect the reliability of LFIA. In summary, natural enzymes still possess certain advantages in the field of LFIA signal amplification. Nonetheless, the influence of test samples and detection conditions on them must be taken into account.

3.2. Nanozyme-based signal amplification strategies

Nanozymes are believed to serve as catalytic cores for signal amplification processes due to enzyme activity similar to natural enzymes. Nanozymes are simple in preparation, tunable in catalytic activity, low in cost, large in surface area, and strong in the ability to resist environmental effects [87,88]. After decades of research, many different types of nanozymes were developed, including noble metals [69,89], transition metal oxides [90,91], transition metal sulfide [92,93], carbon materials [94-96], and MOFs [97,98]. By designing the composition and structure, nanozymes can realize the coexistence of multiple properties [72-74]. In LFIA, nanozymes can be used to provide efficient catalytic amplification and introduce signals for calibration and analyte detection needs. This review summarizes the applications of nanozymes, including noble metal, non-noble metal, and composite nanozymes, that are used in LFIA.

3.2.1. Noble metal nanozymes

As well known, AuNPs are the most commonly used noble metal in LFIA [99]. Despite being widely present, there are few in-depth reports in academic research due to their relatively weak enzymatic activity. In contrast, noble metal nanoparticles of Pt [69], Pd [100], Ru [101], Ir [102], *etc.* exhibit excellent POD-like activity, becoming a current research hotspot. Li *et al.* synthesized Pt-Ru bimetallic nanoclusters (NCs) with high POD-like activity [69]. Their specific activity exceeded monometallic Pt NCs and some reported single-atom nanozymes. Analysis showed that Ru deposition hindered Pt crystal growth to form nanoclusters with subparticle microstructures and rich interfaces (Fig. 5a), resulting in POD-like activity enhancement. Superior activity was caused by electron transmission from Ru to Pt atoms, which was confirmed by density functional theory (DFT) calculations and X-ray photoelectron spectroscopy (XPS) (Fig. 5b). The application of this highly active Pt-Ru probe in LFIA detection of D-dimers amplifies the visual signal by 100 times, demonstrating its potential application in bioanalysis.

Meng *et al.* successfully applied double-layer Pd@Ir bimetallic nanozymes to LFIA detection of pepsinogen I and II for ultrasensitive cancer diagnosis [70]. In this study, it was proven that the energy barrier of the rate-determining step for Pd@Ir NPs was significantly lower than that of monometallic Pd and Ir NPs (Figs. 5c and d), thus accelerating the production of ·OH (Fig. 5e), and improving catalytic efficiency. Ultimately, the LOD as low as 0.05 ng/mL for pepsinogen I/II was achieved. Separately, Seong *et al.* synthesized porous Pt NPs for sensitive C-reactive protein LFIA detection [1]. Utilizing a three-dimensional fluidic setup (Fig. 5f) and

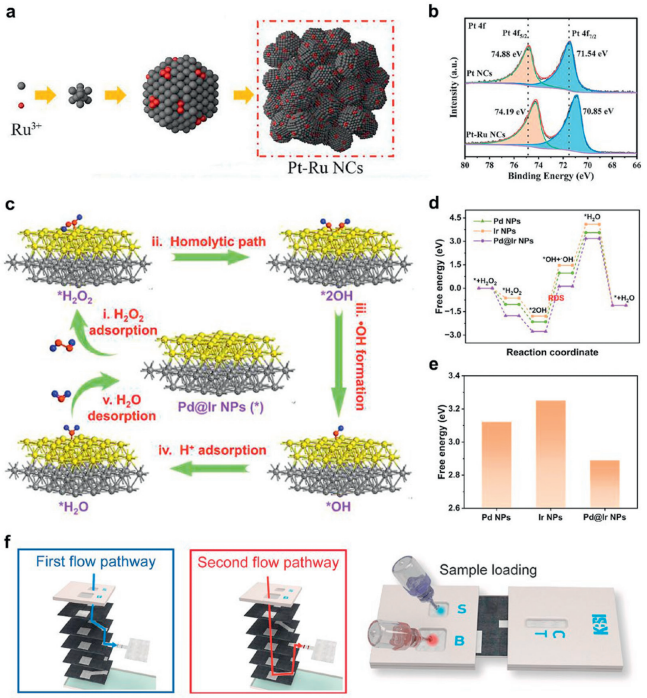

Fig. 5. (a) Schematic diagram of influence of Ru atom hindrance on the ordered growth of Pt crystals. (b) XPS spectra for Pt 4f in different NCs. Reproduced with permission [69]. Copyright 2023, Elsevier B.V. (c) Proposed catalytic mechanism of Pd@Ir NPs for H_2O_2-induced ·OH production in an acidic environment. (d) Free energy diagrams of Pd@Ir NPs during catalysis. (e) Reaction energy barrier of ·OH dissociation from different samples. Reproduced with permission [70]. Copyright 2023, American Chemical Society. (f) Schematic diagram of three-dimensional fluidic configuration. Reproduced with permission [1]. Copyright 2023, Elsevier B.V.

diaminobenzidine for signal amplification, they achieved a detection limit of 0.03 ng/mL in just 20 min.

Need to mention, noble metals possess abundant free electrons and stable chemical states, which are ideal candidates for efficient catalytic reactions. There are many strategies to enhance enzymatic activity, such as modulating the electronic structure of noble metals with bonding atoms or molecules, influencing the electron distribution on the surface of noble metals through ligands, and harnessing the hot electrons and holes generated by the plasmonic resonance effect. On the one hand, these strategies contribute to reducing the usage of noble metals and lowering costs, on the other hand, open up broad prospects for research on the enhancement mechanisms of composite enzymes by combining noble metals with other nanostructures.

3.2.2. Non-noble metal nanozyme

Despite numerous reports exploring the application of noble metal nanozymes in LFIA, the primary focus is on the exceptional enzymatic activity exhibited by noble metal nanoparticles. However, non-noble metal nanozymes have also been found to possess abundant activity enhancement strategies [103-105], and inherent diverse properties have been shown to offer expanded possibilities for LFIA detection. Cai *et al.* innovatively developed Fe-N-C single-atom nanozymes for highly sensitive LFIA detection of mycotoxins [28]. Hemin was doped into ZIF-8 to produce Fe-N-C nanozymes *via* thermal decomposition. The hemin amount influenced ZIF-8 size and structural stability, thereby optimizing the POD-like activity of the nanozymes. The Fe-N-C probes interacted with sample antigens to form probe-antigen complex, which was captured by the T/C line. The introduction of H_2O_2 and TMB triggered catalytic oxidation, resulting in a bright blue band (Fig. 6a). XPS analysis showed pyridinic-N and graphitic-N as the main N species, which

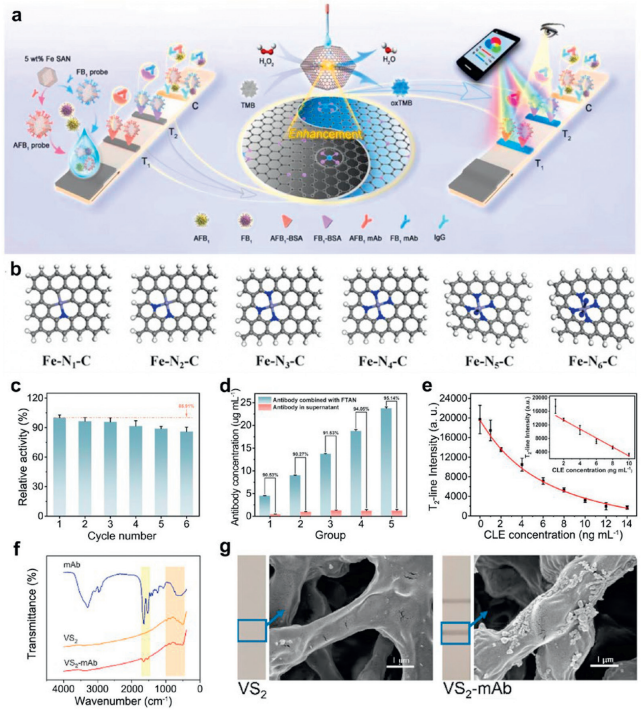

Fig. 6. (a) Signals amplification mechanism of Fe-N-C nanozymes in LFIA. (b) Six DFT calculation models with various coordination environments. Reproduced with permission [28]. Copyright 2022, Elsevier B.V. (c) Reusability of Fe-based tannic acid nanozymes. (d) Evaluation of the coupling efficiency of FTAN-antibody (Groups 1–5: antibody concentration of 5, 10, 15, 20, and 25 μg/mL). (e) Regression equations of catalytic signal for clenbuterol. Reproduced with permission [6]. Copyright 2022, Elsevier B.V. (f) FTIR spectra of different samples. (g) The scanning electron microscope image of the VS_2-based and VS_2-mAb-based LFIA. Reproduced with permission [29]. Copyright 2022, American Chemical Society.

were the main factor of enhancing the Fe-N_x site catalytic activity. Fig. 6b displays six Fe-N_x configurations from DFT calculations. X-ray absorption spectroscopy confirmed the effective confinement of Fe atoms in the nanozymes. DFT revealed that the Fe-N_4 structure was the lowest formation energy structure, increased ·OH detachment effectivity and higher reaction rates. Highly sensitive LFIA detections of aflatoxin B1 and fumonisin B1 were achieved with limits of 2.8 and 13.9 pg/mL, respectively.

Inspired by mussels, Liu *et al.* used tannic acid, a renewable resource with strong metal ion chelating and biomolecular affinity, to create a Fe-based nanozyme (FTAN) [6]. Prepared *via* a formaldehyde-assisted crosslinking method, FTAN showed remarkable stability (Fig. 6c) and allowed simple antibody conjugation (Fig. 6d). FTAN nanozymes were integrated into LFIA and amplified colorimetric signals (Fig. 6e), achieving the detection of ractopamine and clenbuterol at 0.015 and 0.156 ng/mL, respectively. Separately, Chen *et al.* employed 2D VS_2 nanosheets as enzymatic labels in LFIA for sensitive 17β-estradiol detection [29]. The VS_2 nanosheets with advantages over HRP in catalytic activity, stability, and adsorption capacity, which could spontaneously adsorb antibodies without crosslinking agents (Figs. 6f and g). Due to the monolayer structure, VS_2 nanosheets exhibited enhanced Coulomb interactions, reduced screening effects, and a large exciton effect, all of which confer VS_2 with excellent POD-like activity. The signal-enhanced LFIA based on VS_2 nanosheets achieved a low detection limit of 0.065 ng/mL for 17β-estradiol within 7 min.

Compared to noble metal nanozymes, non-noble metal nanozymes have lower costs and can be structured for various applications. Activity optimization can enhance the detection performance of enzyme-based LFIA. Designing nanozymes tailored for LFIA catalytic environment may boost signal amplification. An in-depth analysis of the nanozyme structure-activity relationship, revealing their enzyme-like mechanisms, is the crucial future research direction that guides nanozyme optimization and application. Nanozymes serve as excellent probes for enzymatic signal amplification in LFIA. However, their enzymatic activity relies on exposed surface structures, which are vulnerable to deactivation by ligands in the solution. Additionally, ion concentration to the sample solution was limited due to nanozymes colloidal instability.

3.2.3. Composite nanozymes

Nanozymes are obtained through simple chemical preparation and possess various inherent properties such as optics, thermodynamics, and electromagnetics, which provide the possibility for achieving composite signal LFIA based on nanozyme modified probes. Hence, these inherent properties, which are resilient to interferences, can be introduced as calibration signals to correct for errors arising from factors such as ambient temperature and solution environment, thereby enhancing the stability and reliability of detection results [39]. In the reports of photothermal and colorimetric composite-signal LFIA, most colorimetric signals originate from the inherent color of the label, with only a few being derived from the amplification of enzyme activity. Among them, Liang *et al.* designed a copper-anchored polydopamine (PCu) formed by the copolymerization of copper ions and dopamine as a multimodal nanozymes label for LFIA detection of aflatoxin [71]. The copper ion in this label provides good POD-like activity, and the excellent photothermal conversion capability derived from the polydopamine (PDA) scaffold. Therefore, the PCu label can provide triple signal readings of colorimetry signal, amplified colorimetry signal, and photothermal signal (Fig. 7a). The existing form of copper in PCu is a mixture of CuO, Cu_2O, and Cu^0. Additionally, the POD-like activity and photothermal conversion performance of PCu were investigated. Based on the triple signal readings of the PCu nanozymes, LFIA achieved highly sensitive detection of aflatoxin, with detection limits for colorimetric and photothermal signals as low as 0.45 and 0.22 ng/mL, respectively.

In other immunosensing platforms, multimodal signals have emerged as a novel design strategy. First, Wang *et al.* reported a Co-doped graphitic carbon nitride (Co-doped g-C_3N_4) with POD-like activity and photoluminescence properties for dual-mode detection of hypoxanthine [72]. The nanozyme was coupled with xanthine oxidase to oxidize the chromogenic substrate OPD to *o*-phthaldialdehyde with yellow fluorescence. Thus, the colorimetric signal of the solution and the fluorescence ratio (F_{570}/F_{370}) were used as dual-mode signals for high-precision quantification of hypoxanthine. Additionally, both the groups of Zhang and Cai developed two composite nanozymes based on Prussian blue (Au@PBNP and AuAg@PB MOF) for enhancing colorimetric and surface enhanced Raman scattering (SERS) dual-mode sensing [73,74]. The composite structures were formed between noble metals and Prussian blue (PB) by self-assembled sheet growth (Fig. 7b). The colorimetric signal was enhanced by the ultra-high POD-like activity of PB, and the Raman signal was amplified by the noble metal core (Figs. 7c and d).

Composite nanozymes are expected to become one of the important development directions for the next generation of LFIA labels. The detection accuracy of the LFIA platform can be improved through the combination of high-precision rapid detection signals with high-stability instrument detection signals while meeting the need for preliminary qualitative detection in limited conditions for POCT. In sensing platforms such as ELISA and solution detection, have been reports of "multi-in-one" labels. Therefore, the LFIA platform can be further developed by modifying and adapting the above composite signal labels.

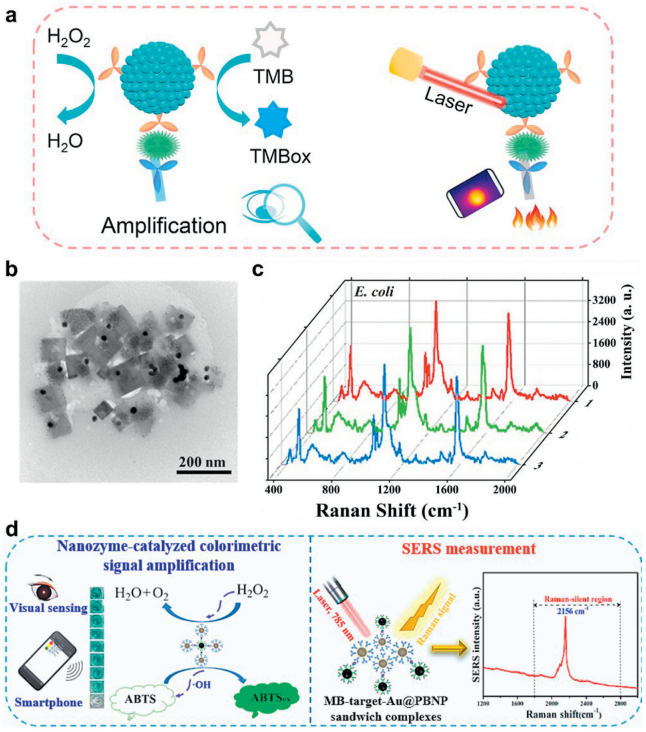

Fig. 7. (a) Mechanism for the POD-like colorimetric and photothermal multimodal analysis of *A. flavus*. Reproduced with permission [71]. Copyright 2022, Elsevier B.V. (b) TEM image of Ag-etched Au@Ag NP caused by adding $K_3[Fe(CN)_6]$. (c) The 3 randomly selected SERS spectra acquired from nanozyme-based sandwich system for *E. coli*. Reproduced with permission [73]. Copyright 2023, Elsevier B.V. (d) Principle of the colorimetric/SERS dual-readout immunoassay based on a bifunctional Au@PBNP nanozyme for detection of food allergic proteins. Reproduced with permission [74]. Copyright 2023, Elsevier Ltd.

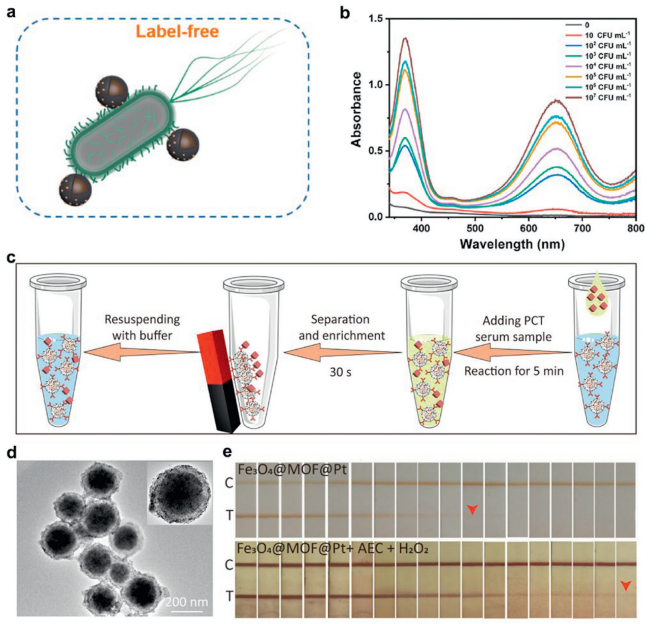

Fig. 8. (a) Label-free strategy based on the interaction of Fe_3O_4@PDA@Pt and *E. coli* O157:H7. (b) Absorbance spectra of the Fe_3O_4@PDA@Pt nanocomposite-mediated catalytic reaction with different concentrations of *E. coli* O157:H7. Reproduced with permission [58]. Copyright 2022, Elsevier B.V. (c) Schematic diagram of magnetic enrichment method. (d) TEM image of Fe_3O_4@MOF@Pt. (e) Photographs of Fe_3O_4@MOF@Pt-labeled test strips in response to different concentrations of PCT before and after catalysis. Reproduced with permission [59]. Copyright 2022, American Chemical Society.

Because of the significant cost advantages over natural enzymes, nanozymes are considered as a suitable candidate for developing LFIA platforms with low profit margins. More importantly, the process of linking the nanozymes to recognition devices, such as antibodies and aptamers, required no cumbersome purification step, greatly shortening the development cycle of the new LFIA. Simultaneously, the inherent properties of nanozymes afford the possibility for the generation of composite signals, and their self-calibration capabilities offer a promising avenue of research for the development of highly accessible and precise LFIA. Hence, in the development of high-precision quantitative LFIA, nanozymes are considered as highly potential materials for the preparation of immunoprobes. Their diverse properties provide researchers with flexible options, thereby being utilized to accommodate the specific demands of various analytes. In addition, some reports have involved indirect strategies derived from nanozymes, which can also achieve amplification of LFIA signals.

4. Indirect enzyme-based signal amplification strategies

In direct signal amplification strategies for LFIA, natural enzymes or nanozymes probes are employed as catalytic cores for the rapid oxidation of substrates, generating high-intensity color signals and thereby achieving the goal of signal amplification. However, in certain special cases, such as requiring a wide linear range, low affinity of recognition elements, or significant sample interference with the flow, direct signal amplification strategies may not meet these demands. Consequently, indirect signal amplification strategies utilizing enzymes have been developed by researchers. Pre-enrichment effectively separates the analyte from complex samples, eliminating potential interference from the sample during the chromatography process and significantly enhancing detection sensitivity [58,59]. Furthermore, by constructing cascade reactions, a broader detection range can be achieved through multi-step signal amplification mechanisms [75,106,107].

4.1. Sensitivity enhancement strategies by pre-enrichment

The pre-enrichment strategy for samples involves separating the probe analyte complex using the magnetic properties of the probe, followed by resuspending the purified complex to obtain a concentrated sample solution for chromatography, ultimately enhancing the detection sensitivity of LFIA. The implementation of pre-enrichment techniques in samples presents a viable approach for enhancing the sensitivity of lateral flow immunoassay. Dou *et al.* designed the composite nanozymes with a Fe_3O_4 core modified with a PDA layer and Pt nanoparticles (Fe_3O_4@PDA@Pt) [58]. The Fe_3O_4 magnetic core assisted analyte concentration. PDA film was used to adhere strongly to pathogenic bacteria (Fig. 8a), and POD activity was induced *via* Pt nanoparticle deposition, which boosted the signal (Fig. 8b). This allowed Fe_3O_4@PDA@Pt nanozymes to detect *E. coli* O157:H7 without antibodies. Premixing the probe with the sample, followed by magnetic separation after bacteria adsorption, this strategy achieved an LOD of 10 colony-forming units (CFU)/mL and a detection range of 10–10^7 CFU/mL after signal amplification.

Furthermore, Chen *et al.* successfully prepared a trifunctional composite nanozyme with a Fe_3O_4 core, an outer layer of MIL-100(Fe), and Pt nanoparticles embedded in the outermost layer [59]. The typical magnetic pre-enrichment process involves mixing magnetic probes with the sample, followed by the separation of probe-analyte complexes from the mixture using magnetism, and their resuspension in a working buffer for subsequent chromatographic analysis (Fig. 8c). Its three-layer structure exhibited ultra-high POD-like activity due to synergistic effects between MIL-

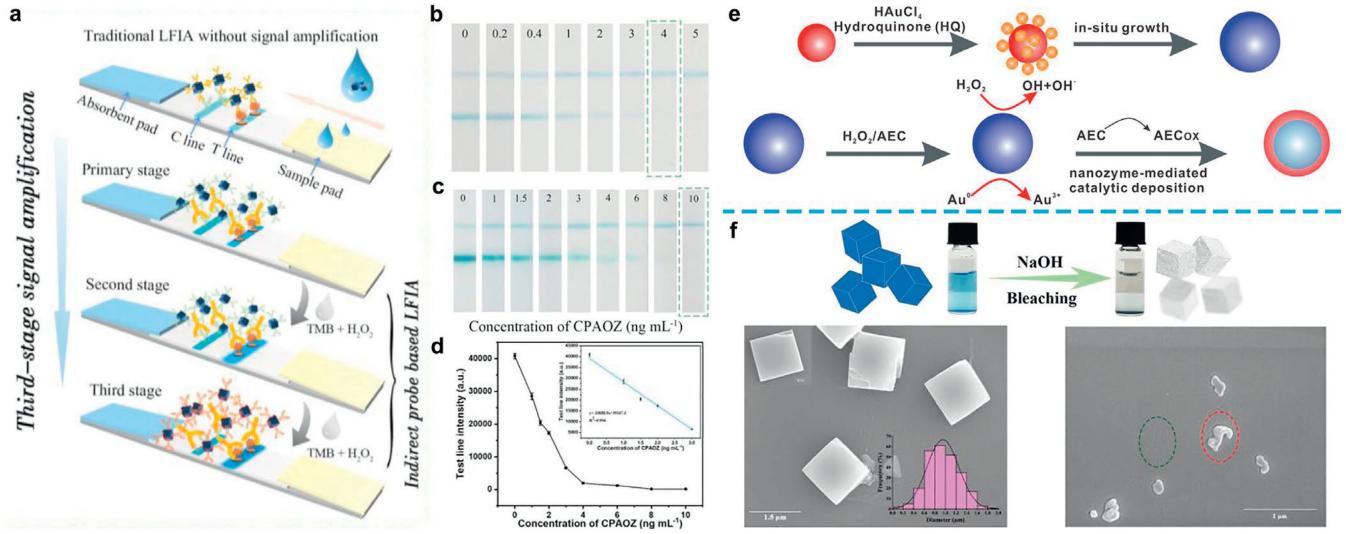

Fig. 9. (a) Illustration of the signal amplification based on the third-stage amplifier indirect probe strategy. Assay results for antigen of various concentrations *via* the indirect probe based LFIAs (b) before catalysis and (c) after catalysis. (d) Test line intensity corresponding to CPAOZ concentration by TsAIP-based LFIA after catalysis, inside: calibration curve of CPAOZ assay. Reproduced with permission [75]. Copyright 2021, Elsevier Ltd. (e) Principle and analysis of the enhanced AuNP-ICA method for *E. coli* O157:H7 detection using the proposed two-step cascade signal amplification. Reproduced with permission [62]. Copyright 2020, American Chemical Society. (f) The PBNCs degradation after reaction with NaOH solution and Scanning electron microscopy images of before and after reaction. Reproduced with permission [61]. Copyright 2020, Elsevier Ltd.

101(Fe) and Pt NPs (Fig. 8d), enabling highly sensitive LFIA detection of procalcitonin (PCT) in human serum with a detection limit of 0.5 pg/mL (Fig. 8e).

Furthermore, Ren *et al.* reported a multifunctional nanozymes probe that integrates colorimetric, catalytic, and magnetic functionalities for the detection of 17β-estradiol [60]. The probes were formed by modifying antibodies on the surface of $NiCo_2O_4$ nanoparticles and eliminated the need for complex multilayer coating. The LFIA based on $NiCo_2O_4$ achieved a detection limit of 0.2 ng/mL for 17β-estradiol. The design efficiently mitigates matrix effects from food samples, thereby enhancing both detection sensitivity and stability.

4.2. Cascade reactions amplification strategies

In signal amplification strategies for LFIA, a cascade reaction system is created by generating or conjugating enzymatic activity units on captured probes, enhancing enzymatic activity, and amplifying the signal. Due to nitrocellulose membrane pore size limitations, large labels can hinder probe movement, restricting enzyme label size in LFIA. *In situ* deposition of metals like Au, Ag, and Cu after chromatography or nanozymes can amplify the signal. Ren *et al.* [75] reported a three-level amplification LFIA using PB for furazolidone detection. Fig. 9a showed the three-level amplification strategy: PB nanoparticles with goat-anti-mouse IgG (H + L) antibody (GAMA) linked to monocloning antibody (mAb) for the first amplification, PB nanozymes catalyze TMB and H_2O_2 for the second, and HRP-connected GAMA catalyze TMB oxidation for the third. This strategy lowered the furazolidone detection limit to 1 ng/mL and doubled the detection range (Figs. 9b–d), showcasing cascade signal amplification advantages in LFIA.

Fu *et al.* achieved two-step signal amplification in LFIA for sensitive *E. coli* O157:H7 detection using *in situ* Ag deposition and nanozyme-catalyzed deposition [62]. $HAuCl_4$ was used to form a POD-like shell on AuNPs, amplifying the colloidal gold signal. Nanozyme catalyzed H_2O_2 and AEC for further amplification (Fig. 9e). This reduced the detection limit to 12.5 CFU/mL with just 75 µL of sample. On the contrary, for competitive LFIA, amplifying signal reduction is preferred. Bu *et al.* reported an amplification strategy by PB degradation using NaOH, increasing signal reduction and achieving a 23 pg/mL aflatoxin B1 detection limit (Fig. 9f) [61]. Guo *et al.* used composite nanozymes as "nanomotors" to enhance antigen-antibody binding in LFIA, improving sensitivity to 2.2 ng/mL for pepsinogen I/II detection [108].

The indirect signal amplification strategy utilizing enzymes is founded upon meticulously designed enzymatic mechanisms and the inherent characteristics of nanozymes. This tailored approach is frequently developed for the detection of specific analytes, rendering it challenging to be directly applied to other analytes for LFIA detection. Hence, when devising indirect amplification strategies, emphasis must be placed not only on their potent signal amplification capabilities but also on ensuring generality. However, enzymatic signal amplification as a general method also needs to fine-tune the appropriate enzyme catalytic system according to the characteristics of the analytes and the source of samples, to ensure the best catalytic effect and required sensitivity.

5. Conclusion, challenges, and outlook

The LFIA technology has matured and is backed by a robust research and design framework. Enzyme-catalyzed signal amplification has proven effective in boosting LFIA sensitivity, without major changes to production or usage conditions. Natural enzymes, with their diverse activities, facilitate novel amplification methods. Nanozymes, as amplification labels, leverage their composite capabilities, offering efficient amplification, diverse signals, and cascade reactions, thereby strengthening signals and decreasing LFIA conditions, broadening its application scope.

Despite progress, challenges remain. Strategy precision depends on stable enzyme activity, which is affected by changes in the sample-induced catalytic environment. Nanozyme stability research is limited. The high cost and complex steps of natural enzymes hinder their LFIA use. Existing strategies partially address these but have drawbacks like low loading efficiency and activity shielding. Nanozymes production and modification are straightforward, but external conditions affect their activity, specially pH value. Current LFIA amplification mostly relies on POD-like activity, overlooking natural enzyme diversity.

In analysis, the key challenges are balancing detection sensitivity, false positives, and assay selectivity. Most studies have improved specificity but often omitted methodology details. Additionally, maintaining signal stability after amplification remains challenging. Different reaction termination methods exist, from substrate diffusion in clear water to using terminating agents like dilute sulfuric acid or sodium dodecyl sulfate. However, most studies choose not to terminate the reaction, measuring signal intensity at fixed time points. Since these factors are pivotal for LFIA industrial application, future research must comprehensively balance these factors to the design of high-performance LFIA.

In enzyme-based LFIA signal amplification, the detection time is crucial. The majority of LFIA techniques complete analysis within 30 min (Table 1). Direct amplification strategies can shorten amplification time to 1 min [29,69,71]. However, long-term stability and reproducibility of LFIA over 6 months are rarely studied, and the probe stability in solution was explored by some researchers [6,69,70]. In LFIA industrialized production, test strip stability is the key index. Thus, strategies for enhancing performance must consider all conditions, not just signal amplification. Enzyme label design and choice of materials for probes and test strips are equally important.

In addition to the design of the enzyme label, the choice of substrate also plays a crucial role in signal amplification performance. Diaminobenzidine has been found to reduce reaction speed in certain systems [109], while OPD exhibits poor stability in the liquid phase, necessitating its use under dark conditions. Although AEC demonstrates good stability, its sensitivity is relatively low. It is worth noting that all these substrates possess certain toxicity. On the other hand, TMB stands out due to its excellent stability, sensitivity, and high extinction capability of its dark blue product, making it a preferred choice for signal amplification. However, given the selectivity of nanozymes towards substrates, the screening of substrates plays a significant role in enhancing signal amplification performance. Therefore, when selecting a substrate, comprehensive consideration must be given to its properties and compatibility with enzymes.

To address the current challenges, several potential directions of development have been identified. Firstly, developing enzyme probes with enhanced activity and stability is fundamental for efficient colorimetric signal amplification, thereby boosting practical utility. Secondly, exploring enzyme labels with composite signals provides self-calibration, preserving LFIA ease of use and detection accuracy by selecting interference-resistant calibration references. Furthermore, optimizing signal amplification methods and leveraging enzymes unique properties can improve selectivity and reduce background noise, resulting in enhancing LFIA signal recognizability. Lastly, designing signal amplification protocols aligned with LFIA practical scenarios optimizes and streamlines detection processes, augmenting LFIA practicality and applicability. This review aims to refine enzyme-based signal amplification strategies, advancing LFIA application in high-sensitivity rapid detection, ultimately offering a guideline for the development of high-precision LFIA in disease monitoring, food safety, environmental protection, and other fields.

Declaration of competing interest

The authors declare that they have no known competing financial interests or personal relationships that could have appeared to influence the work reported in this paper.

CRediT authorship contribution statement

Haijiang Gong: Writing – original draft, Conceptualization. **Qingtan Zeng:** Writing – original draft. **Shili Gai:** Writing – review & editing. **Yaqian Du:** Software. **Qingyu Wang:** Writing – original draft. **He Ding:** Writing – review & editing. **Lichun Wu:** Writing – review & editing. **Anees Ahmad Ansari:** Writing – review & editing. **Piaoping Yang:** Writing – review & editing.

Acknowledgments

Financial supports from the National Natural Science Foundation of China (NSFC, Nos. 52272144 and 22205048), Heilongjiang Provincial Natural Science Foundation of China (No. JQ2022E001), China Postdoctoral Science Foundation (Nos. 2022M710931 and 2023T160154), Heilongjiang Postdoctoral Science Foundation (No. LBH-Z22010), Natural Science Foundation of Shandong Province (No. ZR2020ZD42), and the Fundamental Research funds for the Central Universities are greatly acknowledged.

References

[1] S.E. Son, S.H. Cheon, W. Hur, et al., Biosens. Bioelectron. 243 (2024) 115752.
[2] P. Tripathi, A. Kumar, M. Sachan, et al., Biosens. Bioelectron. 165 (2020) 112368.
[3] H. Chen, X. Ma, X. Zhang, et al., Chin. Chem. Lett. 34 (2023) 107701.
[4] H. Zhao, E. Su, L. Huang, et al., Chin. Chem. Lett. 33 (2022) 743–746.
[5] X. Yin, J. Hou, J. Guo, et al., Chem. Eng. J. 469 (2023) 143979.
[6] S. Liu, R. Shu, J. Ma, et al., Chem. Eng. J. 446 (2022) 137382.
[7] S. Liu, X. He, T. Zhang, et al., Chin. Chem. Lett. 33 (2022) 1933–1935.
[8] Y. Liu, T. Li, G. Yang, et al., Chin. Chem. Lett. 33 (2022) 1913–1916.
[9] W. Li, Z. Wang, X. Wang, et al., J. Environ. Chem. Eng. 11 (2023) 110494.
[10] M. Tian, W. Xie, T. Zhang, et al., Sens. Actuators B: Chem. 309 (2020) 127728.
[11] M. Song, J. Xing, H. Cai, et al., ACS Nano 17 (2023) 10748–10759.
[12] N. Yao, X. Li, Y. Tian, et al., Sens. Actuators B: Chem. 379 (2023) 133247.
[13] E. Renzi, A. Piper, F. Nastri, et al., Small 19 (2023) 2207949.
[14] G. Li, Q. Li, X. Wang, et al., Int. J. Biol. Macromol. 242 (2023) 125186.
[15] Y. Liu, L. Zhan, Z. Qin, et al., ACS Nano 15 (2021) 3593–3611.
[16] J. Liu, M. Li, Q. Man, et al., Anal. Chem. 95 (2023) 8011–8019.
[17] W. Qiao, B. He, J. Yang, et al., Int. J. Biol. Macromol. 254 (2024) 127746.
[18] A.R. Gul, J. Bal, P. Xu, et al., Biosens. Bioelectron. 246 (2024) 115902.
[19] C. Lu, W. Xiao, Y. Su, et al., ACS Sens. 8 (2023) 1950–1959.
[20] X. Ruan, V. Hulubei, Y. Wang, et al., Biosens. Bioelectron. 208 (2022) 114190.
[21] J. Xu, L. Dou, S. Liu, et al., Food Chem. 352 (2021) 129415.
[22] J. Feng, Y. Xue, X. Wang, et al., Sci. Total Environ. 834 (2022) 155354.
[23] E.Y. Kwon, X. Ruan, F. Yu, et al., Food Chem. 399 (2023) 133955.
[24] Y. Chen, L. Fan, W. Deng, et al., J. Infect. 85 (2022) 702–769.
[25] E.I. Newsham, E.A. Phillips, H. Ma, et al., Lab Chip 22 (2022) 2741–2752.
[26] P. Srithong, S. Chaiyo, E. Pasomsub, et al., Microchim. Acta 189 (2022) 386.
[27] A.H. Iles, P.J.W. He, I.N. Katis, et al., Talanta 248 (2022) 123579.
[28] X. Cai, F. Ma, J. Jiang, et al., J. Hazard. Mater. 441 (2023) 129853.
[29] Y. Chen, J. Ren, X. Yin, et al., Anal. Chem. 94 (2022) 8693–8703.
[30] J. Hu, X. Xu, L. Xu, et al., Food Biosci. 51 (2023) 102353.
[31] J. Liang, Z. Liu, Y. Fang, et al., Food Chem. 417 (2023) 135897.
[32] L. Zhu, Z. Lu, L. Zhang, et al., Chin. Chem. Lett. 33 (2022) 2491–2495.
[33] Z. Ren, L. Xu, L. Yang, et al., Anal. Chem. 95 (2023) 6646–6654.
[34] X. Zhang, J. Wang, J. Liang, et al., Food Chem. 390 (2022) 133188.
[35] S. Tao, X. Zhao, D. Bao, et al., ACS Appl. Mater. Interfaces 15 (2023) 27612–27623.
[36] X. Yang, X. Cheng, H. Wei, et al., J. Nanobiotechnology 21 (2023) 450.
[37] Z. Xie, S. Feng, F. Pei, et al., Anal. Chim. Acta 1233 (2022) 340486.
[38] M. Hussain, X. Liu, J. Zou, et al., Chin. Chem. Lett. 33 (2022) 1885–1888.
[39] X. Liu, X. Su, M. Chen, et al., Biosens. Bioelectron. 245 (2024) 115840.
[40] J. Wang, Y. Zheng, X. Wang, et al., Sci. Total Environ. 912 (2024) 169440.
[41] C. Lin, Z. Liu, F. Fang, et al., ACS Sens. 8 (2023) 3733–3743.
[42] B. Wang, T. Peng, Z. Jiang, et al., ACS Sens. 8 (2023) 4512–4520.
[43] G. Wang, L. Wang, Z. Meng, et al., Adv. Fiber Mater. 4 (2022) 1304–1333.
[44] Z. Guo, B. Jin, Y. Fang, et al., Chin. Chem. Lett. 33 (2022) 4208–4212.
[45] A. Sena-Torralba, Y.D. Banguera-Ordoñez, L. Mira-Pascual, et al., Trends Biotechnol. 41 (2023) 1299–1313.
[46] B. Fang, Q. Xiong, H. Duan, et al., Trends Analyt. Chem. 157 (2022) 116754.
[47] J. Wu, X. Wang, Q. Wang, et al., Chem. Soc. Rev. 48 (2019) 1004–1076.
[48] C. Parolo, A.d.l. Escosura-Muñiz, A. Merkoçi, Biosens. Bioelectron. 40 (2013) 412–416.
[49] G.B. Aktas, J.H. Wichers, V. Skouridou, et al., Microchimica Acta 186 (2019) 426.
[50] V.G. Panferov, I.V. Safenkova, A.V. Zherdev, et al., Talanta 225 (2021) 121961.
[51] F. Chai, D. Wang, L. Zhu, et al., Anal. Chem. 94 (2022) 6628–6634.
[52] Y. Chen, J. Sun, Y. Xianyu, et al., Nanoscale 8 (2016) 15205–15212.
[53] Z. Huang, S. Zhou, X. Wang, et al., Sens. Actuators B: Chem. 385 (2023) 133699.
[54] H. Wang, C. Yao, J. Fan, et al., Biosens. Bioelectron. 237 (2023) 115508.
[55] Y. Chen, K. Tang, Q. Zhou, et al., Anal. Chem. 95 (2023) 18139–18148.
[56] C. Zhou, R. Cheng, B. Liu, et al., Sens. Actuators B: Chem. 402 (2024) 135118.
[57] P. Nie, X. Gao, X. Yang, et al., Food Chem. 439 (2024) 138122.

[58] L. Dou, Y. Bai, M. Liu, et al., Biosens. Bioelectron. 204 (2022) 114093.
[59] R. Chen, X. Chen, Y. Zhou, et al., ACS Nano 16 (2022) 3351–3361.
[60] J. Ren, X. Yin, H. Hu, et al., Sens. Actuators B: Chem. 367 (2022) 132150.
[61] T. Bu, F. Bai, X. Sun, et al., Food Chem. 344 (2021) 128711.
[62] J.H. Fu, Y. Zhou, X. Huang, et al., J. Agric. Food. Chem. 68 (2020) 1118–1125.
[63] S. Li, Y. Zhang, Q. Wang, et al., Anal. Chem. 94 (2021) 312–323.
[64] F. Arshad, S.N.A. Zakaria, M.U. Ahmed, Food Chem. 438 (2024) 137947.
[65] J. Li, P. Liang, T. Zhao, et al., Anal. Bioanal. Chem. 415 (2023) 545–554.
[66] O.D. Hendrickson, E.A. Zvereva, A.V. Zherdev, et al., Food Control. 133 (2022) 108655.
[67] R. Zhao, Y. Tang, D. Song, et al., Anal. Chem. 95 (2023) 18522–18529.
[68] J. Xu, M. Wang, M. Li, et al., Anal. Chim. Acta 1279 (2023) 341834.
[69] X. Li, C. Qian, Y. Tian, et al., Chem. Eng. J. 457 (2023) 141324.
[70] X. Meng, W. Zuo, P. Wu, et al., Nano Lett. 24 (2023) 51–60.
[71] M. Liang, X. Cai, Y. Gao, et al., Biosens. Bioelectron. 213 (2022) 114435.
[72] X. Wang, C. Hong, Z. Lin, et al., Food Sci. Hum. Well. 13 (2024) 879–884.
[73] J. Cai, Y. Lin, X. Yu, et al., Sens. Actuators B: Chem. 394 (2023) 134279.
[74] X. Zhang, Y. Shi, D. Wu, et al., Food Chem. 434 (2024) 137455.
[75] J. Ren, L. Su, H. Hu, et al., Food Chem. 377 (2022) 131920.
[76] D. Hui, Z. Jiangyan, W. Yating, et al., Anal. Chem. 96 (2024) 1789–1794.
[77] Z. Zhang, N. Zhu, Y. Zou, et al., Anal. Chim. Acta 1035 (2018) 168–174.
[78] D. Xu, J. Zhang, Z. Luo, et al., Food Chem. 439 (2024) 138125.
[79] M.S. Chang, C.Y. Lee, E.S. Liu, et al., Anal. Chem. 95 (2023) 14341–14349.
[80] Y.C. Chen, J.J. Chen, Y.J. Hsiao, et al., Sens. Actuators B: Chem. 336 (2021) 129725.
[81] Q. Zhao, D. Lu, G. Zhang, et al., Talanta 223 (2021) 121722.
[82] Shtenberg Nirala, Biomolecules 9 (2019) 372.
[83] Y. Zhang, X. Liao, G. Yu, et al., Anal. Chem. 95 (2023) 13698–13707.
[84] L.H. Ma, H.B. Wang, T. Zhang, et al., Sens. Actuators B: Chem. 298 (2019) 126819.
[85] W. Pengcheng, S. Jiaren, S. Caixia, et al., Trends Analyt. Chem. 166 (2023) 117203.
[86] Y. Chang, Q. Zhang, W. Xue, et al., Chem. Commun. 59 (2023) 3399–3402.
[87] L. Zhang, X. Bi, X. Liu, et al., Nanoscale 15 (2023) 12853–12867.
[88] Q. Wang, J. Jiang, L. Gao, WIREs Nanomed. Nanobi. 14 (2022) e1769.
[89] J. Chen, X. Liu, G. Zheng, et al., Small 19 (2022) 2205924.
[90] B. Liu, Z. Sun, P.J.J. Huang, et al., J. Am. Chem. Soc. 137 (2015) 1290–1295.
[91] Z. Yi, X. Yang, Y. Liang, et al., Small 20 (2024) 2305974.
[92] X. Yu, Y. Wang, J. Zhang, et al., Adv. Healthc. Mater. 13 (2023) 2302023.
[93] S. Liang, X. Deng, Y. Chang, et al., Nano Lett. 19 (2019) 4134–4145.
[94] D. Zhu, N. Li, M. Zhang, et al., Biosens. Bioelectron. 243 (2024) 115786.
[95] J. Wang, Y. Chu, Z. Zhao, et al., J. Nanobiotechnology 21 (2023) 311.
[96] L. Zhang, L. Xu, Y. Wang, et al., Chin. Chem. Lett. 33 (2022) 4089–4095.
[97] Y. He, M. Feng, X. Zhang, et al., Anal. Chim. Acta 1283 (2023) 341959.
[98] Y. Tang, Y. Han, J. Zhao, et al., Nano-Micro Lett. 15 (2023) 112.
[99] B. Jiang, D. Duan, L. Gao, et al., Nat. Protoc. 13 (2018) 1506–1520.
[100] S. Singh, P. Tripathi, N. Kumar, et al., Biosens. Bioelectron. 92 (2017) 280–286.
[101] Q. Liu, X. Wang, Y. Zhang, et al., Biosens. Bioelectron. 244 (2024) 115785.
[102] G. Yim, C.Y. Kim, S. Kang, et al., ACS Appl. Mater. Interfaces 12 (2020) 41062–41070.
[103] M. Zandieh, J. Liu, ACS Nano 15 (2021) 15645–15655.
[104] Y. Wu, W. Xu, L. Jiao, et al., Mater. Today 52 (2022) 327–347.
[105] Z. Zeng, X. Wang, T. Yang, et al., Anal. Chim. Acta 1245 (2023) 340861.
[106] O.D. Hendrickson, E.A. Zvereva, A.V. Zherdev, et al., Foods 11 (2022) 1691.
[107] W. Peng, Y. Qin, W. Li, et al., ACS Sens. 5 (2020) 1912–1920.
[108] J. Guo, Y. Li, B. Wang, et al., Microchim. Acta 189 (2022) 468.
[109] T. Bai, L. Wang, M. Wang, et al., Biosens. Bioelectron. 208 (2022) 114218.